



HAL
open science

A two-component parameterization of marine ice-nucleating particles based on seawater biology and sea spray aerosol measurements in the Mediterranean Sea

Jonathan Trueblood, Alessia Nicosia, Anja Engel, Birthe Zäncker, Matteo Rinaldi, Evelyn Freney, Melilotus Thyssen, Ingrid Obernosterer, Julie Dinasquet, Franco Belosi, et al.

► To cite this version:

Jonathan Trueblood, Alessia Nicosia, Anja Engel, Birthe Zäncker, Matteo Rinaldi, et al.. A two-component parameterization of marine ice-nucleating particles based on seawater biology and sea spray aerosol measurements in the Mediterranean Sea. *Atmospheric Chemistry and Physics*, 2021, 21 (6), pp.4659-4676. 10.5194/acp-21-4659-2021 . hal-03203880

HAL Id: hal-03203880

<https://hal.science/hal-03203880>

Submitted on 21 Apr 2021

HAL is a multi-disciplinary open access archive for the deposit and dissemination of scientific research documents, whether they are published or not. The documents may come from teaching and research institutions in France or abroad, or from public or private research centers.

L'archive ouverte pluridisciplinaire **HAL**, est destinée au dépôt et à la diffusion de documents scientifiques de niveau recherche, publiés ou non, émanant des établissements d'enseignement et de recherche français ou étrangers, des laboratoires publics ou privés.



Distributed under a Creative Commons Attribution 4.0 International License



A two-component parameterization of marine ice-nucleating particles based on seawater biology and sea spray aerosol measurements in the Mediterranean Sea

Jonathan V. Trueblood¹, Alessia Nicosia¹, Anja Engel², Birthe Zäncker², Matteo Rinaldi³, Evelyn Freney¹, Melilotus Thyssen⁴, Ingrid Obernosterer⁵, Julie Dinasquet^{5,6}, Franco Belosi³, Antonio Tovar-Sánchez⁷, Araceli Rodriguez-Romero⁷, Gianni Santachiara³, Cécile Guieu⁵, and Karine Sellegri¹

¹Université Clermont Auvergne, CNRS, Laboratoire de Météorologie Physique (LaMP) 63000 Clermont-Ferrand, France

²GEOMAR, Helmholtz Centre for Ocean Research Kiel, 24105 Kiel, Germany

³Institute of Atmospheric Sciences and Climate, National Research Council, 40129 Bologna, Italy

⁴Mediterranean Institute of Oceanography, 163 avenue de Luminy, Marseille, France

⁵CNRS, Sorbonne Université, Laboratoire d'Océanographie de Villefranche, UMR7093, Villefranche-sur-Mer

⁶Marine Biology Research Division, Scripps Institution of Oceanography, 92037 La Jolla, CA, USA

⁷Department of Ecology and Coastal Management, Institute of Marine Sciences of Andalusia (ICMAN-CSIC), 07190 Puerto Real, Spain

Correspondence: Karine Sellegri (k.sellegri@opgc.cnrs.fr)

Received: 18 May 2020 – Discussion started: 23 June 2020

Revised: 21 January 2021 – Accepted: 29 January 2021 – Published: 25 March 2021

Abstract. Ice-nucleating particles (INPs) have a large impact on the climate-relevant properties of clouds over the oceans. Studies have shown that sea spray aerosols (SSAs), produced upon bursting of bubbles at the ocean surface, can be an important source of marine INPs, particularly during periods of enhanced biological productivity. Recent mesocosm experiments using natural seawater spiked with nutrients have revealed that marine INPs are derived from two separate classes of organic matter in SSAs. Despite this finding, existing parameterizations for marine INP abundance are based solely on single variables such as SSA organic carbon (OC) or SSA surface area, which may mask specific trends in the separate classes of INP. The goal of this paper is to improve the understanding of the connection between ocean biology and marine INP abundance by reporting results from a field study and proposing a new parameterization of marine INPs that accounts for the two associated classes of organic matter. The PEACETIME cruise took place from 10 May to 10 June 2017 in the Mediterranean Sea. Throughout the cruise, INP concentrations in the surface microlayer (INP_{SML}) and in SSAs (INP_{SSA}) produced using a plunging aquarium apparatus were continuously monitored while surface seawater (SSW) and SML biological properties

were measured in parallel. The organic content of artificially generated SSAs was also evaluated. INP_{SML} concentrations were found to be lower than those reported in the literature, presumably due to the oligotrophic nature of the Mediterranean Sea. A dust wet deposition event that occurred during the cruise increased the INP concentrations measured in the SML by an order of magnitude, in line with increases in iron in the SML and bacterial abundances. Increases in INP_{SSA} were not observed until after a delay of 3 days compared to increases in the SML and are likely a result of a strong influence of bulk SSW INPs for the temperatures investigated ($T = -18\text{ °C}$ for SSAs, $T = -15\text{ °C}$ for SSW). Results confirmed that INP_{SSA} are divided into two classes depending on their associated organic matter. Here we find that warm ($T \geq -22\text{ °C}$) INP_{SSA} concentrations are correlated with water-soluble organic matter (WSOC) in the SSAs, but also with SSW parameters (particulate organic carbon, POC_{SSW} and $\text{INP}_{\text{SSW}, -16\text{C}}$) while cold INP_{SSA} ($T < -22\text{ °C}$) are correlated with SSA water-insoluble organic carbon (WIOC) and SML dissolved organic carbon (DOC) concentrations. A relationship was also found between cold INP_{SSA} and SSW nano- and microphytoplankton cell abundances, indicating that these species might be a source of water-insoluble or-

ganic matter with surfactant properties and specific IN activities. Guided by these results, we formulated and tested multiple parameterizations for the abundance of INPs in marine SSAs, including a single-component model based on POC_{SSW} and a two-component model based on SSA WIOC and OC. We also altered a previous model based on OC_{SSA} content to account for oligotrophy of the Mediterranean Sea. We then compared this formulation with the previous models. This new parameterization should improve attempts to incorporate marine INP emissions into numerical models.

1 Introduction

Ice-nucleating particles (INPs) are a subset of aerosol particles that are required for the heterogeneous nucleation of ice particles in the atmosphere. While extremely rare (Rogers et al., 1998), INPs greatly control the ice content of clouds, which is crucial to a range of climate-relevant characteristics including precipitation onset, lifetime, and radiative forcing (Verheggen et al., 2007). Despite their importance, the knowledge of INP sources and concentrations, particularly in marine regions, remains low as evidenced by the large uncertainties in modelled radiative properties of clouds (McCoy et al., 2015, 2016; Franklin et al., 2013).

While the ice-nucleating (IN) ability of marine SSA particles is less efficient than their terrestrial counterparts (DeMott et al., 2016), modelling studies have shown that marine INPs are of particular importance in part due to the lack of other INP sources in such remote regions (Burrows et al., 2013; Vergara-Temprado et al., 2017). For this reason, recent studies have been conducted to better understand which SSA particles contribute to the marine INP population as well as the relationship between SSA emission and ecosystem productivity. Results from these studies suggest that the IN ability of SSAs is linked to the biological productivity of source waters, with higher productivity leading to greater IN activity (DeMott et al., 2016; Bigg, 1973; Schnell and Vali, 1976). For example, it has been shown that both the cell surface and organic exudate of the marine diatom *Thalassiosira pseudonana* can promote freezing at conditions relevant to mixed-phase clouds (Knopf et al., 2011; Wilson et al., 2015). More recently, mesocosm studies on phytoplankton blooms using two separate in-lab SSA-generation techniques have furthered the understanding of the connection between ocean biology and the IN activity of SSAs (McCluskey et al., 2017). In-depth chemical analysis of the artificially generated SSAs during this set of experiments has revealed marine INPs may be related to two classes of organic matter: a regularly occurring surface-active molecule type related to dissolved organic carbon (DOC) and long-chain fatty acids, and an episodic heat-labile microbially derived type (McCluskey et al., 2018a).

As the understanding of the connection between ocean biology and marine INPs has improved, parameterizations for predicting marine INP abundance using readily available ocean parameters have been proposed. Wilson and co-authors (Wilson et al., 2015) identified a temperature-dependent relationship between TOC and ice-nucleating entity (INE) number concentrations in the surface microlayer (SML) from samples collected in the North Atlantic and Arctic ocean basins. They then extended this relationship from the ocean to the atmosphere to predict the abundance of INPs in SSAs based on model estimates of marine organic carbon aerosol concentrations. The parameterization was tested for the first time on field measurements of marine aerosol over the North Atlantic at Mace Head and was found to overestimate INP abundance in pristine marine aerosols by a factor of 4 to 100 at -15 and -20 °C (McCluskey et al., 2018b). In the same study, a new parameterization based on SSA surface area and temperature was proposed (McCluskey et al., 2018b). However, this parameterization did not incorporate the recently observed heat-labile organic INPs. Most recently, this parameterization was compared with observations of INPs over the Southern Ocean, showing reasonable agreement between predictions and observations at -25 °C (McCluskey et al., 2019).

Despite the recent progress made in the understanding of marine INPs, there remains much room for improvement. To date, previous parameterizations have only been tested in the two field studies mentioned in the previous paragraph, underscoring the need for more real-world observations. Furthermore, the field studies conducted so far have taken place in regions of the ocean where biological productivity is high (i.e. North Atlantic and Southern Ocean). As modelling work has shown that the link between ocean biology and SSA organic content properties in oligotrophic waters differs from those in highly productive regions (Burrows et al., 2014) there is a need for more measurements in waters with low primary productivity. Finally, despite the finding that marine INPs may exist as two separate populations, no model has yet been proposed to account for this.

This paper addresses the current gaps in the knowledge of marine INPs by (1) testing existing parameterizations of INPs on a new set of field measurements by extending the current inventory of field measurements beyond eutrophic waters to more oligotrophic regions for the first time, (2) improving the understanding of how INPs in the SML and SSAs are linked to both seawater biological and SSA organic properties, and (3) proposing a new parameterization based on the two-component nature of INPs. Here we present results from the ProcEss studies at the Air-sEa Interface after dust deposition in the Mediterranean Sea (PEACETIME) cruise. The cruise took place in the central and western Mediterranean Sea from 10 May–10 June 2017. Observations of INP concentrations in both the SML and SSAs were compared with a suite of surface seawater, surface microlayer, and SSA prop-

erties to better determine how INP concentrations related to biology.

2 Methods

In the frame of the PEACETIME project (<http://peacetime-project.org/>, last access: 11 March 2021), an oceanographic campaign took place aboard the French research vessel (R/V) *Pourquoi Pas?* between 10 May–10 June 2017 with the purpose of investigating the processes that occur at the air–sea interface in the Mediterranean Sea. The cruise started in La Seyne, France, and travelled in a clockwise fashion between 35 to 42° latitude and 0 to 20° longitude. The observations and process studies performed on board in both the whole water column and the atmosphere are described elsewhere (Freney et al., 2020). Here, we focus on the measurements conducted to describe the SML, surface seawater (SSW), and aerosol properties.

2.1 Surface seawater (SSW)

SSW properties presented here were obtained from sampling at depths of 20 cm and 5 m. First, 21 parameters including various chemical properties, microbial assemblages, hydrological properties, and optical properties were monitored using the ship's underway system that continuously collected seawater at 5 m under the ship using a large peristaltic pump (Verder VF40 with EPDM hose). These measurements included counts of specific microbial classes (e.g. *Synechococcus*, *Prochlorococcus*, picoeukaryotes, nanoeukaryotes, microphytoplankton, high-phycoerythrin-containing cells, coccolithophores, cryptophytes), as well as seawater biovolume, chlorophyll *a* (chl *a*), and POC concentrations. Chl *a* was determined from the particulate absorption spectrum line height at 676 nm after adjusting to PEACETIME chl *a* from high-performance liquid chromatography (HPLC). POC was estimated from the particulate attenuation at 660 nm using an empirical relationship specific to PEACETIME ($\text{POC} = 1405.1 \times c_p(660) - 52.4$). For enumeration of phytoplankton cells, an automated Cytosense flow cytometer (Cytobuoy, NL) operating at a time resolution of 1 h was connected to the continuous underway seawater system. Particles were carried in a laminar-flow-filtered seawater sheath fluid and subsequently detected with forward scatter and sideward scatter as well as fluorescence in the red (FLR > 652 nm) and orange (FLO 552–652 nm) ranges. Distinction between highly concentrated picophytoplankton and cyanobacteria groups and lower concentrated nano- and microphytoplankton was accomplished using two trigger levels (trigger level FLR 7.34 mV, sampling speed of $4 \text{ mm}^3 \text{ s}^{-1}$ analysing $0.65 \pm 0.18 \text{ cm}^3$ and trigger level FLO 14.87 mV at a speed of $8 \text{ mm}^3 \text{ s}^{-1}$ analysing $3.57 \pm 0.97 \text{ cm}^3$).

The second set of SSW measurements were made on seawater collected at ~ 20 cm depth from a pneumatic boat that

was periodically deployed at a distance of 2 km from the R/V to avoid contamination. The SSW was manually collected using acid-cleaned borosilicate bottles. From these discrete samples, microbial composition and cell abundance of the SSW was monitored as described in a companion paper (Tovar-Sanchez et al., 2019). Measurements included heterotrophic bacteria counts, high nucleic acid and low nucleic acid bacteria (HNA and LNA bacteria, respectively), total non-cyanobacteria-like cells (NCBL), cyanobacteria like cells (CBL), and total phytoplankton concentration (NCBL + CBL). These were further segregated into size classes of small, medium, and large which roughly correspond to the pico-, nano-, and microsize classifications from the underway measurements. Trace metals (i.e. Cd, Co, Cu, Fe, Ni, Mo, V, Zn, Pb) were analysed by inductively coupled plasma mass spectrometry, although here we only report on Fe. Finally the abundance of DOC and marine gel-like particles, including transparent exopolymer particles (TEPs) and Coomassie stainable particles (CSPs), were also measured as described in the literature (Engel, 2009).

2.2 Surface microlayer

At the same time SSW samples were manually collected on the pneumatic boat, SML samples were also collected using a glass plate sampling method which has been previously described in the literature (Tovar-Sanchez et al., 2019). The glass plate was cleaned overnight with acid and rinsed with ultrapure Milli-Q water. Roughly 100 dips of the glass were conducted to collect 500 mL of SML water into 0.5 L acid-cleaned low-density polyethylene plastic bottles. The samples were then acidified on board to pH < 2 with ultrapure-grade hydrochloric acid in a class-100 HEPA laminar-flow hood. The same measurements done for the SSW samples (see above, Sect. 2.1) were then made on the SML samples. Enrichment factor was calculated for relevant properties as the ratio of SML to SSW:

$$\text{EF} = \frac{\text{SML}}{\text{SSW}}. \quad (1)$$

In addition to biological measurements, concentrations of immersion freezing mode INPs in SML samples (and a small number of SSW samples, $n = 4$) were measured between 22 May–7 June using an offline method described previously (Stopelli et al., 2014). Briefly, prior to acidification of the SML samples, additional aliquots were separated and stored in Corning Falcon 15 mL conical tubes and frozen at -20°C until analysis. Before INP measurement, each aliquot was gradually defrosted and distributed into an array of 26 Eppendorf tubes filled up to 200 μL . The array was then immersed inside an LED-based Ice Nuclei Detection Apparatus (LINDA), and the number of ice-nucleating particles per litre (INPL^{-1}) of SML water followed the method described in Stopelli et al. (2014), which was originally formulated by

Vali (1971):

$$\frac{\text{INP}}{\text{volume}} = \frac{\ln(N_{\text{total}}) - \ln(N_{\text{unfrozen}})}{V_{\text{tube}}}, \quad (2)$$

where N_{total} is the total number of tubes, N_{unfrozen} is the total number of unfrozen tubes, and V_{tube} is the volume of sample in each tube. The number of unfrozen tubes is calculated by first blank correcting the number of frozen tubes and then subtracting that value from the total number of tubes. We calculated uncertainty as the binomial proportion confidence interval (95 %) using the Wilson score interval. Samples were not corrected for salinity in this study.

2.3 Artificially generated sea spray aerosol

Sea spray aerosols were generated using a sea spray generation apparatus which has been described previously (Schwier et al., 2015; Schwier et al., 2017). The characteristics of the setup were selected to mimic Fuentes et al. (2010). These parameters (water flow rates, plunging water depth, etc.) have been shown to mimic nascent SSAs well. The apparatus consists of a 10 L glass tank with a plunging jet system. A continuous flow of seawater collected at 5 m depth using the ship's underway seawater circulating system (described above) was supplied to the apparatus. Particle-free air was passed perpendicular to the water surface at a height of 1 cm to send a constant airflow across the surface of the water. Aerosols were then either dried with a 1 m long silica dryer for on-line instrumentation (see Sect. 2.3.3), with a 30 cm silica gel dryer cascade impactor sampling with subsequent chemical analysis, or were sampled directly from the sea spray generator onto filters for INP analysis.

2.3.1 Offline PM1 filter analysis

Aerosol particles were also sampled onto PM1 quartz fibre filters mounted on a four-stage cascade impactor (10 L min^{-1}) on a daily basis (24 h duration). Samples were then extracted in Milli-Q water by sonication for 30 min for the analysis of water-soluble components. The main inorganic ion abundance (i.e. SO_4^{2-} , NO_3^- , NH_4^+ , Na^+ , Cl^- , K^+ , Mg^{2+} , Ca^{2+}) was analysed via ion chromatography. An IonPac CS16 3×250 mm Dionex separation column with gradient methanesulfonic acid elution was used for cations, while an IonPac AS11 2×250 mm Dionex column with gradient potassium hydroxide elution was used for anions. Water-soluble organic carbon (WSOC) and water-insoluble organic carbon (WIOC) were also determined. WSOC was measured after water extraction using a high-temperature catalytic oxidation instrument (Shimadzu; TOC 5000 A). Total organic carbon (which we now refer to as OC) was measured using a Multi N/C 2100 elemental analyser (Analytik Jena, Germany) with a furnace solids module. The analysis was performed on an 8 mm diameter filter punch, pre-treated with $40 \mu\text{L}$ of H_3PO_4 (20 % v v⁻¹) to remove contributions

from inorganic carbon. WIOC was determined as the difference between OC and WSOC. Finally, we calculated organic mass fraction of SSA (OMSS) by taking the ratio of OM / (OM + SeaSalt), where OM is the sum of WSOM and WIOM, calculated as $\text{WSOM} = \text{WSOC} \times 1.8$ and $\text{WIOM} = \text{WIOC} \times 1.4$, and SeaSalt is the sum of inorganic ion abundance as determined above.

2.3.2 INPs

INP concentrations were determined from filter-based samples of total suspended particles over a 24 h duration daily or from the average of two filters (day and night). The volume sampled on each filter averaged $8.95 \times 10^3 \pm 2.26 \text{ m}^3$ of air. The concentration of INPs in the SSAs was determined for the condensation freezing mode using a Dynamic Filter Processing Chamber (DFPC), which has been used in multiple previous studies and found to agree well with other INP monitoring instruments (DeMott et al., 2018; Hiranuma et al., 2019; McCluskey et al., 2018b). A full description of the instrument can be found in the literature (DeMott et al., 2018). Briefly, bulk SSAs formed using the plunging aquarium apparatus were impacted onto 47 mm nitrocellulose filters which were then placed on a metal plate coated with a smooth surface of Vaseline. Air entered the chamber and was sent through a cooling coil allowing it to become saturated with respect to water. Different supersaturations with respect to ice and liquid water can be obtained by controlling the temperatures of the filter and the air flowing across the filter. Filter air temperature combinations were set three different ways, all resulting in a supersaturation with respect to liquid water of 1.02. The filter temperatures were -18 , -22 , and -25 °C (-15.9 , -19.6 , and -22.3 °C for air temperature). Under these conditions, condensation freezing is expected to be the dominant freezing mode for INPs. It has been reported (Vali et al., 2015) that condensation freezing and immersion freezing are not distinguishable from one another. Filters were processed inside the DFPC for 15 min and monitored for formation of ice crystals upon activation of INPs. Based on sampling time and flow rate, the number of INPs per volume were calculated. We report an uncertainty of ± 30 % based on previous reports of the DFPC (DeMott et al., 2018).

2.3.3 Size distribution measurements

Particle size distribution and number concentrations of aerosols generated with the plunging apparatus were monitored using a custom-made differential mobility particle sizer (DMPS) preceded by a $1 \mu\text{m}$ size-cut impactor and X-ray neutralizer (TSI Inc.). Total counts from the DMPS system were checked using a condensation particle counter (CPC, TSI3010). Using the DMPS, a total of 25 size bins ranging between 10–500 nm (dry particle electrical mobility diameter) were scanned over a 10 min time period. We then aver-

aged the size distributions across each DFPC sampling period. Comparison of the total CPC-based SSA number concentration to the SSA number concentration derived from the DMPS revealed near unity, indicating nearly all of the particle number concentrations were captured by the DMPS. While studies typically present INP concentrations normalized by total SSA surface area, this was not possible in our experiment as the size distribution of supermicrometre particles was not monitored. However, in the supporting information, we do present a theoretical surface area normalized INP_{SSA} calculation for comparison with other studies. The theoretical distribution was based on in situ particle number concentration measurements at Mace Head and open-ocean eddy correlation flux measurements from the Eastern Atlantic (Table S1 in the Supplement; Ovadnevaite et al., 2014), with the resulting surface area distribution shown in Fig. S1 in the Supplement.

3 Results

3.1 INPs in the seawater and SSAs

Ice-nucleating particle characteristics were determined for the SSW, SML, and SSAs. Figure 1a shows the concentration of INPs in the SML (INP_{SML}) at two different temperatures (-12 , -15 °C) and in the SSW (INP_{SSW}) at -15 °C as determined using the LINDA instrument. An initial increase in INP_{SML} occurred on 24 May ($1.8 \times 10^3 \text{ INP L}^{-1}$ at $T = -15$ °C) relative to 22 May which was then followed by a further increase on 4 June ($1.1 \times 10^4 \text{ INP L}^{-1}$ at $T = -15$ °C). The enhancement on 4 June occurred on the same day as a dust deposition event which led to an enrichment of iron in the SML relative to the underlying water (see Sect. 3.2). While only four SSW samples were analysed for INP concentrations, they exhibited similar concentrations and trends to those seen in the SML, with an observed maximum on 4 June ($2.4 \times 10^3 \text{ INP L}^{-1}$ at $T = -15.0$ °C). Based on these four samples, no significant enrichment of INPs was observed in the SML compared to SSW, except during the dust deposition event when the SML concentration was enriched by a factor of 4.5.

Figure 1b shows the concentration of ice-nucleating particles in SSAs (INP_{SSA}) normalized by SSA particle concentration for particles with diameters between 0.1 and 0.5 μm at three different temperatures as observed by the DFPC. It should be noted that INP_{SSA} measurements were conducted at colder temperatures than for the INP_{SML} measurements due to differences between the LINDA and DFPC instruments. In general, the highest concentrations of INP_{SSA} were observed at the beginning of the voyage, with an initial value of $4.0 \times 10^{-9} \text{ INP}_{\text{SSA}, -25^\circ\text{C}} \text{ SSA}^{-1}$ observed on 13 May, increasing to a maximum observed value of $1.3 \times 10^{-8} \text{ INP}_{\text{SSA}, -25^\circ\text{C}} \text{ SSA}^{-1}$ on 20 May. After May 20, a considerable drop in $\text{INP}_{\text{SSA}, -25^\circ\text{C}}$ con-

centrations was observed. Concentrations remained low, albeit with slight fluctuations, before increasing again to $5.2 \times 10^{-9} \text{ INP}_{\text{SSA}, -25^\circ\text{C}} \text{ SSA}^{-1}$ on 7 June. It is also worth noting that the highest concentrations of INPs active at -18 °C ($\text{INP}_{\text{SSA}, -18^\circ\text{C}} \text{ SSA}^{-1}$) were observed on this day. The increase in INP concentrations around the time of the dust deposition event in early June is similar to the trend observed for seawater INPs, albeit with a lag of at least 1 d (no observations of INP_{SSA} were made on 6 June).

Figure 2 shows the comparison of observed INP concentrations at various temperatures in the SML and SSW with those reported in previous studies. The concentrations we report here are lower than those from Arctic seawater samples reported by Irish et al. (2017, 2019) and from Arctic and North Atlantic seawater samples reported by Wilson et al. (2015). The difference can likely be attributed to the fact that eutrophic Arctic and North Atlantic seawater is more biologically active than the oligotrophic Mediterranean Sea. Our values agree well with those reported by Gong et al. (2020) who calculated INP concentrations in mid-latitude seawater off the coast of Cabo Verde. The authors of that study also posited that the low INP concentrations relative to Irish et al. (2017, 2019) and Wilson et al. (2015) were due to the lower biological activity of the oligotrophic seawater near Cabo Verde. As we did not measure the size distribution of particles larger than 500 nm, we cannot directly compare our INP_{SSA} abundance to values cited in previous studies, where concentrations are typically normalized by SSA surface area which is dominated by supermicrometre particles. However, we were able to calculate a theoretical surface area distribution for particles between 0.5–10 μm based on previous studies. The resulting surface area normalized INP concentrations and comparison with literature values is shown in the supporting information (Fig. S2 in the Supplement).

3.2 Correlations between INP and biogeochemical conditions

As described in the methods section, various seawater biogeochemical properties were monitored throughout the voyage for the SSW and SML. Plots of selected continuous measurements from the R/V's underway sampling system and discrete measurements from the pneumatic boat of relevant biogeochemical values are found in the supporting information (Figs. S3 and S4 in the Supplement, respectively). Biogeochemical properties are described in more detail in our companion papers (Guieu et al., 2020a; Tovar-Sanchez et al., 2019), and seawater gel properties will be discussed in an upcoming paper. Here, we present a broad summary of observed conditions.

In general, surface waters were characterized by oligotrophic conditions as expected for the season. Bacteria concentrations ranged between 2×10^5 and $7 \times 10^5 \text{ cells mL}^{-1}$ in the SSW and were greatest at the start and end periods of the voyage. NCBL abundance followed a similar trend and

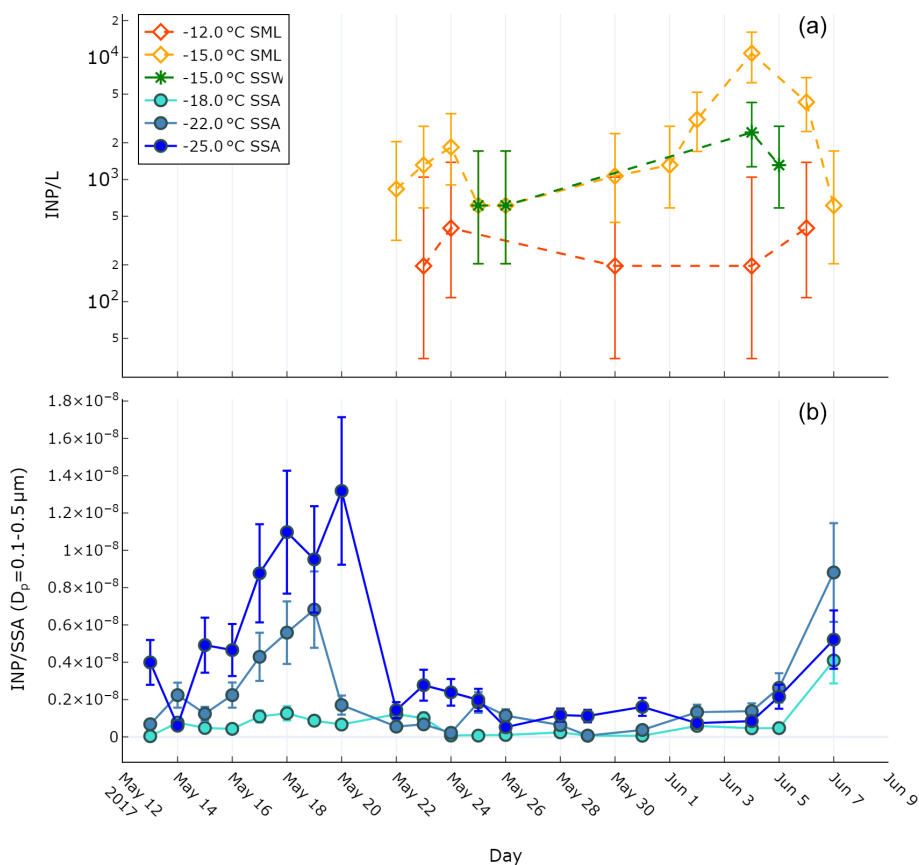


Figure 1. (a) INP concentrations observed during the PEACETIME cruise in the SML and SSW as measured using the LINDA instrument. Error bars represent the binomial proportion confidence interval (95 %) using the Wilson score interval. (b) INP_{SSA} concentrations as observed by the DFPC normalized by SSA particle number concentration. Error bars represent $\pm 30\%$ uncertainty of the DFPC instrument, as cited previously (DeMott et al., 2018).

ranged between 4.0×10^2 – 4.0×10^3 cells mL⁻¹. Observed DOC values ranged between 700–900 μgCL^{-1} and POC values between 42–80 μgCL^{-1} , and these were within the range of expected values for the oligotrophic Mediterranean (540–860 μgCL^{-1} for DOC and 9.6–104 μgCL^{-1} for POC; Pujó-Pay et al., 2011). SSW TEP concentrations ranged between 1.2×10^6 and 1.1×10^7 particles L⁻¹, with CSP between 5.6×10^6 and 9.3×10^6 particles L⁻¹, and will be discussed in a future paper.

Enrichment factors (EFs) in the SML relative to the SSW remained low with an average of 1.10 for DOC, 1.07 for bacteria, and 1.17 for NCBL. As POC was not measured in the SML, we cannot report its EF. TEP was typically enriched relative to the SSW, with an average EF of 4.5, while CSP EF was on average 2.7. Of importance, the dust deposition event that occurred on 4 June led to a drastic increase in SML dissolved iron relative to the SSW (EF ~ 800). This deposition event had important impacts on the biology of the surface seawaters, which is the focus of another paper (Freney et al., 2020). As a result, TEP EF increased to 17, bacteria EF increased to 1.5, and NBCL EF to 2.4. We next discuss

the correlations between INP abundances and biogeochemical properties in the following sections.

3.2.1 Correlations between INP_{SML} abundance and seawater properties

Table 1 shows the correlation statistics between INP_{SML, -15 °C} and selected observed seawater properties (SSW and SML), calculated either for all days of the PEACETIME experiment or only for days before the dust deposition event (i.e. days before 4 June). Relationships are only listed in Table 1 if they were significant ($p < 0.05$) for either all days or pre-dust-only days. Figure 3 shows the corresponding scatterplots of INP_{SML, -15 °C} abundance and SSW properties. We note a statistically significant correlation between INP_{SML, -15 °C} and CSP ($r = 0.87$) as measured from the underway system. When considering only days before the dust deposition event, INP_{SML, -15 °C} is significantly correlated with HNA bacteria ($r = 0.83$) while the correlation with CSP is no longer statistically significant. INP_{SML, -15 °C} are actually negatively correlated with most of the measured SSW properties either when excluding the

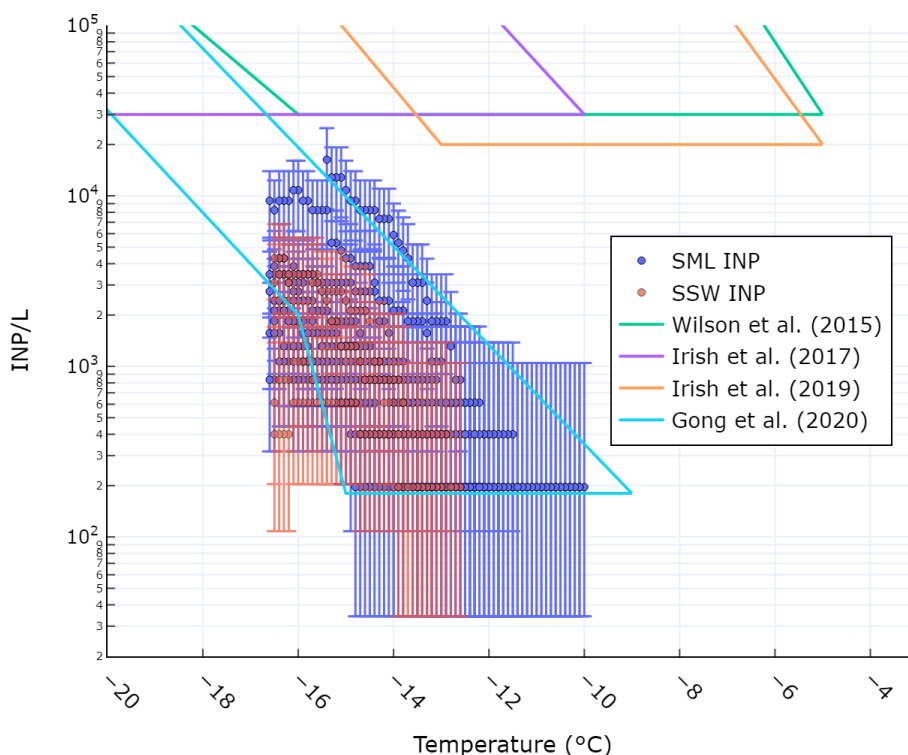


Figure 2. Comparison of observed SSW (blue markers) and SML (red markers) INP concentrations with previous studies. Error bars represent the binomial proportion confidence interval (95 %) using the Wilson score interval.

dust event (for micro-NCBL_{SSW} and TEP_{SSW}) or due to the dust event (for TOC_{SSW}, DOC_{SSW}, and nanoeukaryote cell abundances). This points to a non-proportional transfer of each species from the bulk seawater to the SML relative to one another. Given the high p values and weak correlation coefficients, it is likely that INP_{SML} is not strongly driven by the properties of the underlying SSW. Rather, we posit that INPs in the SML are dictated by SML properties, as shown in the following paragraph.

Figure 4 shows scatterplots of statistically significant relationships between INP_{SML, -15°C} concentrations and various SML properties. INP_{SML, -15°C} is most strongly positively correlated with dissolved iron ($r = 0.99$), TEP EF ($r = 0.95$), and bacteria EF ($r = 0.93$). However, these relationships are skewed by the outlier due to the drastic increase in iron observed on 4 June (Fig. S2a) from the dust deposition event, as described previously. It is difficult to discriminate between the dust and biological impact on the INP_{SML, -15°C}, as dust is known to have good INP properties while also being capable of fertilizing the surface ocean with dissolved iron, leading to concomitant increases in biological activity. It is also possible that the dust deposition led to increased abundance of terrestrial OC, which would exhibit different INP activity. When considering days before the dust event, INP_{SML, -15°C} is only significantly correlated with dissolved iron ($r = 0.91$) and TOC in the SML ($r = -0.93$). We note that while no longer statistically signif-

icant for pre-dust days, moderate correlations were still observed between INP_{SML, -15°C} and total NCBL ($r = 0.48$), HNA bacteria ($r = 0.78$), and total bacteria ($r = 0.64$). Previous reports examining the correlation between INP and microbial abundance have yielded mixed results. For example, a report of INPs in Arctic SML and SSW found no statistically significant relationship between the temperature at which 10 % of droplets had frozen and bacteria or phytoplankton abundances in bulk SSW and SML samples (Irish et al., 2017). However, recent mesocosm studies using nutrient-enriched seawater found that INP abundances between -15 and -25 °C in the aerosol phase were positively correlated with aerosolized bacterial abundance (McCluskey et al., 2017).

A previous study by Wilson and co-authors presented an INP parameterization (hereafter termed W15) based on a positive relationship between seawater TOC and INP abundance in Arctic, North Pacific, and Atlantic SML and SSW (Wilson et al., 2015). Total organic carbon in the SML (TOC_{SML} µgCL⁻¹), derived here as the sum of POC in the SSW (POC_{SSW}) and DOC in the SML (DOC_{SML}), was poorly correlated with INP_{SML, -15°C} ($r = 0.31$, $p = 0.50$). Figure 5 shows the observed INP_{SML, -15°C} / TOC_{SML} ratio (INPs per gram of TOC) for various temperatures and days of the experiment compared with the W15 parameterization (grey line). Our results show observed INP_{SML} / TOC_{SML} ratios below those expected by the model proposed by W15,

Table 1. Correlation statistics between $\text{INP}_{\text{SML},-15^\circ\text{C}}$ and seawater properties in the SML and SSW, where p is the p -value test for significance and r is the Pearson correlation coefficient. Values in parentheses are calculated for days before the dust deposition event (i.e. days before 4 June). Values that are not statistically significant ($p > 0.05$) are italicized.

Variable	$P_{\text{all days}}$ ($P_{\text{pre-dust}}$)	$r_{\text{all days}}$ ($r_{\text{pre-dust}}$)
SSW		
CSP	0.005 (0.78)	0.87 (−0.15)
TOC_{SSW}	0.015 (0.36)	−0.85 (−0.53)
DOC_{SSW}	0.045 (0.52)	−0.76 (−0.39)
Nanoeukaryotes < 10 μm	0.038 (0.20)	−0.63 (−0.51)
Micro-NCBL	0.051 (0.021)	−0.70 (−0.88)
TEP	0.25 (0.022)	−0.46 (−0.88)
Bacteria HNA	0.14 (0.043)	0.57 (0.83)
SML		
Dissolved iron	0.0000021 (0.012)	0.99 (0.91)
TEP EF	0.00032 (0.42)	0.95 (0.41)
Total bacteria EF	0.00075 (0.82)	0.93 (−0.12)
CSP	0.0053 (0.25)	0.87 (−0.56)
Total NCBL	0.0053 (0.34)	0.87 (0.48)
Pico-NCBL	0.0088 (0.43)	0.84 (0.40)
Total Bacteria	0.016 (0.17)	0.81 (0.64)
Phytoplankton (NCBL + CBL)	0.021 (0.68)	0.78 (−0.22)
NCBL EF	0.022 (0.92)	0.78 (0.054)
DOC EF	0.041 (0.38)	0.78 (−0.51)
Nano-NCBL	0.027 (0.42)	0.77 (0.41)
Bacteria HNA	0.012 (0.068)	0.83 (0.78)
Bacteria LNA	0.037 (0.54)	0.74 (0.32)
TOC_{SML}	0.50 (0.020)	0.31 (−0.93)

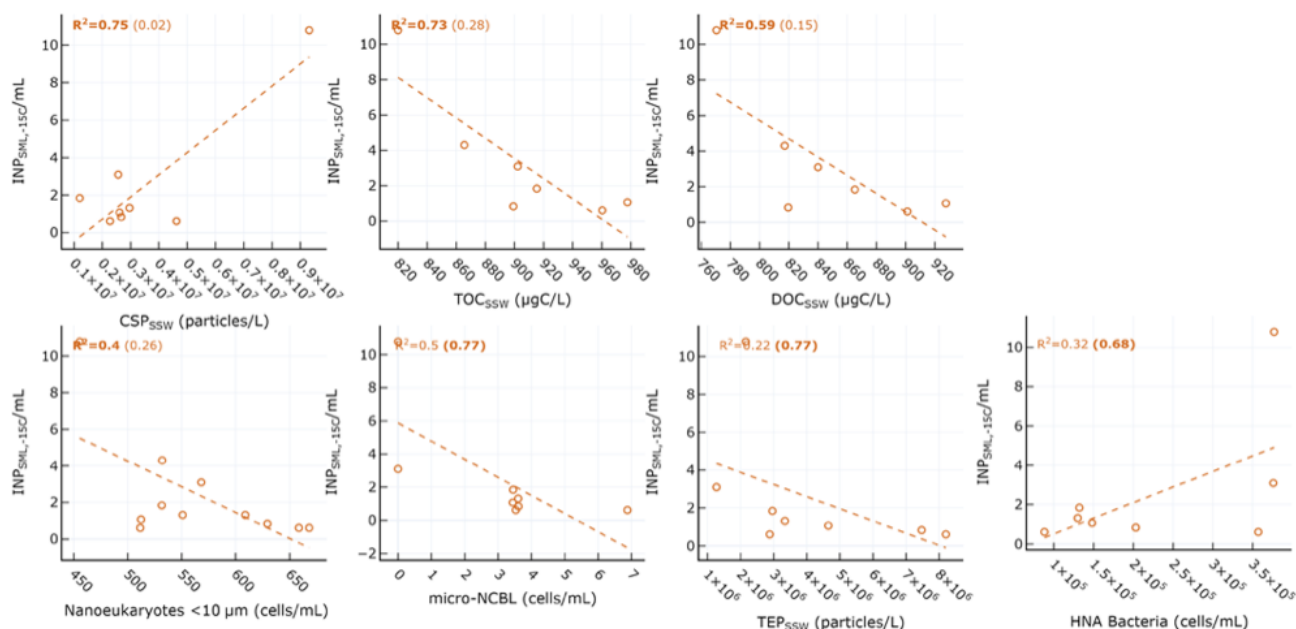


Figure 3. Scatter plot of INPs in the SML and various biogeochemical parameters in the SSW. R^2 for all days are shown in each plot, with R^2 calculated for only days before the dust event shown in parentheses. Statistically significant relationships are shown in bold.

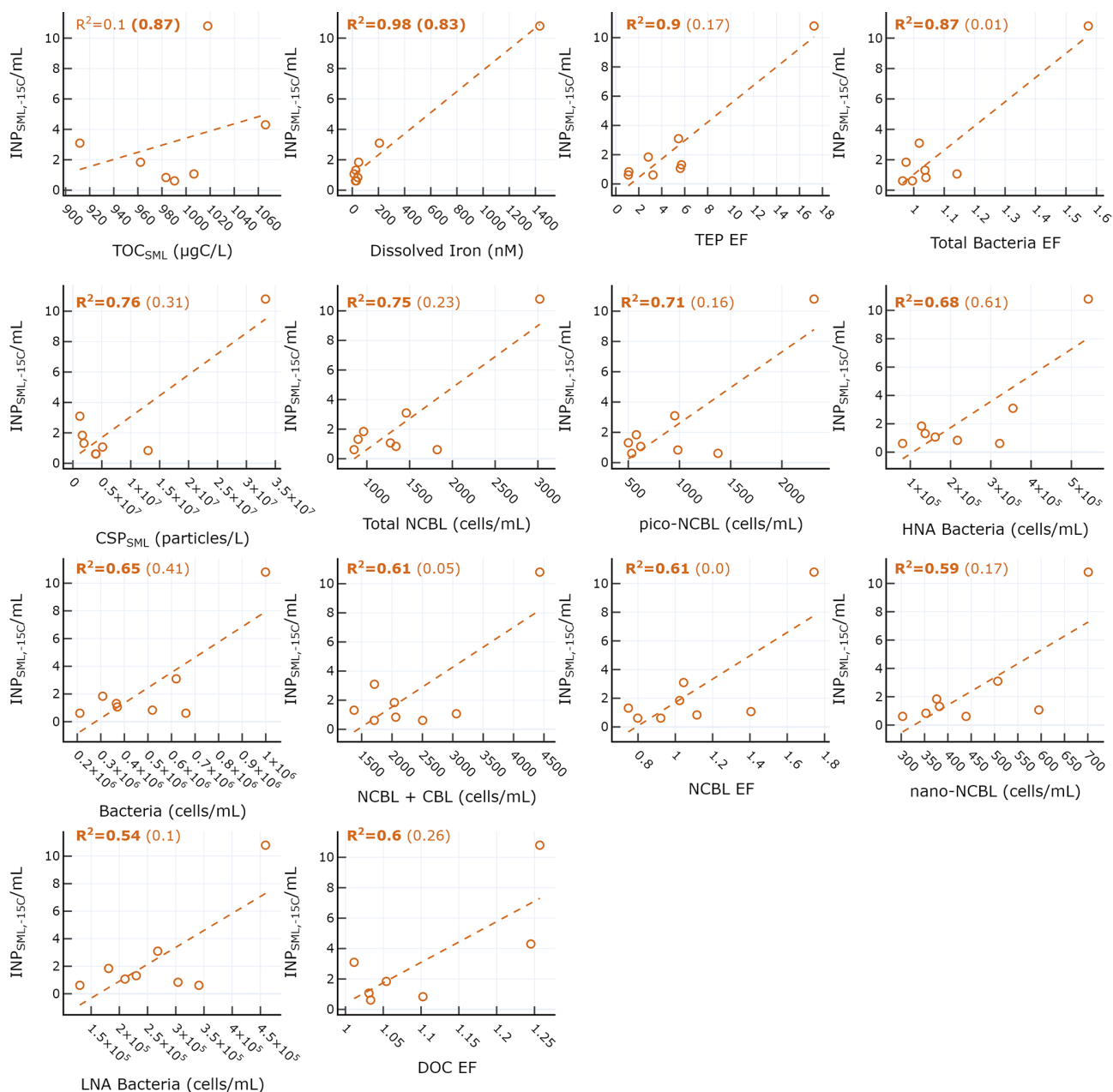


Figure 4. Scatter plot of INPs in the SML and various biogeochemical properties in the SML. R^2 for all days are shown in each plot, with R^2 calculated for only days before the dust event shown in parentheses. Statistically significant R^2 values are shown in bold.

indicating the TOC_{SML} in Mediterranean waters is less IN active at these temperatures than predicted by the W15 parameterization.

In agreement with our findings, a recent study found that the W15 model overpredicted observed INP concentrations in the aerosol phase during two separate mesocosm experiments (McCluskey et al., 2017) by assuming the INP/TOC ratio in the SML was preserved in the aerosol phase. The authors of that study speculated that the overprediction by the W15 model was due to the fact that it does not account

for the complex transfer mechanism of organic matter from the SML to the aerosol phase. Our results here show that the overprediction by W15 persists even when calculating INPs in the SML and therefore the overprediction may be due to other factors beyond the transfer of organic matter from the SML to the atmosphere. We stress, however, that the TOC value used in this study was derived using DOC_{SML} and POC_{SSW} values as POC measurements in the SML were not conducted. As there typically exists an enrichment of organic matter in the SML relative to the bulk seawater, it is possi-

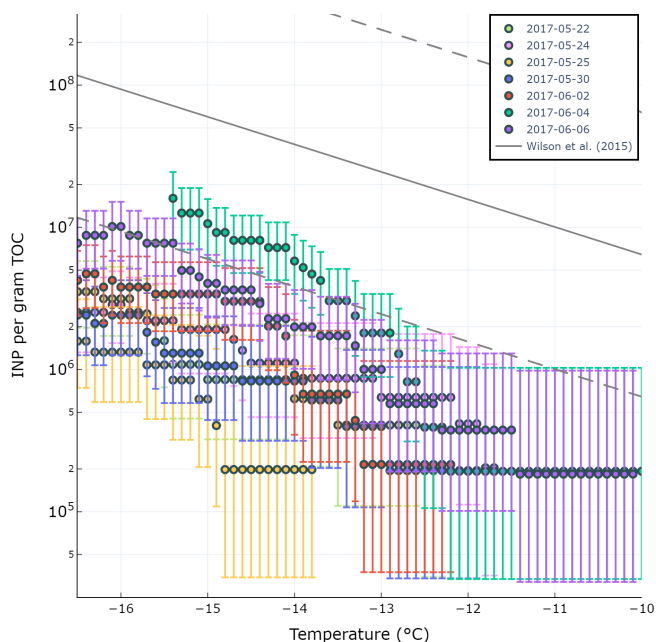


Figure 5. Observed INP/TOC ratio in the SML during PEACE-TIME experiment for different temperatures. The grey line is the fit from Wilson et al. (2015).

ble that the POC_{SSW} we used to calculate TOC_{SML} was below the actual POC content in the SML, thus underestimating TOC_{SML} . However, if this was the case, a higher abundance of TOC_{SML} would only further increase the overprediction of W15 relative to our observations. Finally, it is possible that the oligotrophic nature of Mediterranean waters results in a pool of TOC with a different chemical composition than what is observed in more biologically productive waters such as the Arctic and Atlantic. For example, the pool of TOC during this study was dominated by DOC and featured low POC content, presumably due to low biological productivity.

In summary, $\text{INP}_{\text{SML}, -15^\circ\text{C}}$ increased with SML microbial cell counts (e.g. NCBL and heterotrophic bacteria), Fe_{SML} , and DOC_{EF} during a dust deposition event but was overall not correlated with TOC nor DOC in the SML. Compared to previous studies, the INP/TOC ratio observed in the Mediterranean is low. We surmise that the overprediction of INP/TOC by the model may either be caused by a different relationship between INPs and TOC at warmer temperatures or possibly be due to the chemical characteristics of TOC in the oligotrophic Mediterranean. This complicated relationship between seawater TOC and INP_{SML} highlights the need for further studies focused on the chemical composition of DOC and POC in bulk SSW and SML. Further experiments during low and high biological productivity are needed in controlled environments to better determine under what conditions (oligotrophic and eutrophic) and location in the water column (i.e. bulk SSW vs. SML) TOC, bacteria, and phytoplankton are linked to INPs across a range of temperatures.

Finally, regardless of the exact mechanism, the impact of dust deposition on $\text{INP}_{\text{SML}, -15^\circ\text{C}}$ is fairly large, as we observe an increase in $\text{INP}_{\text{SML}, -15^\circ\text{C}}$ by almost an order of magnitude during the dust event. This impact may have climate implications if $\text{INP}_{\text{SML}, -15^\circ\text{C}}$ were efficiently transferred to the sea spray.

3.2.2 Correlations between INP_{SSA} abundance and observed SSAs and seawater conditions

In the following section, we compare INP_{SSA} at various temperatures with seawater and SSA properties. Sub-micrometre particle concentrations ranged between 1000–3000 particles cm^{-3} (Fig. S5 in the Supplement), and its dependence on seawater biology is further explored in a separate paper (Sellegri et al., under revision). For comparison with seawater properties, INP_{SSA} was first normalized by SSA particle concentration ($0.1 < D_p < 0.5 \mu\text{m}$).

Table 2 shows the correlation statistics between INP_{SSA} normalized by SSA particle number concentration and select conditions in the SML for relationships that were statistically significant. Figure 6 shows the corresponding scatter plots for these relationships. We also tested for correlations on days not affected by the dust event (i.e. days before 4 June), and their statistics are shown in parentheses in Table 2 and Fig. 6. Surprisingly, there were no significant correlations between $\text{INP}_{\text{SSA}, -18^\circ\text{C}}$ and conditions in the SML, including TEP and CSP abundance and enrichment factors, bacteria abundance and enrichment factors and nor with INP_{SML} as measured by the LINDA instrument. This is somewhat unexpected considering INPs in the SML at -15°C were correlated with SML phytoplankton and bacteria counts, which are all expected to transfer efficiently from the SML to the aerosol phase, an assumption widely used in the modelling community. Similarly, -22°C INP_{SSA} had no significant correlations with SML variables, except for TEP EF which was positively correlated ($r = 0.69$) when only considering days before the dust deposition event. At -25°C , INP_{SSA} was found to be significantly correlated with DOC_{SML} and TOC_{SML} on all days ($r = 0.82$ and $r = 0.80$ for DOC and TOC, respectively). When examining only pre-dust-event days, the significant correlations included DOC enrichment as well as nano- and micro-CBL.

Table 3 and the corresponding scatter plots in Fig. 7 show that a weak correlation exists between INP_{SSA} active at -18°C and POC_{SSW} for all days but becomes significant and strong for days not including the dust event. This points to the possible interference of a different class of organic carbon (e.g. terrestrial OC) or the introduction of some other IN-active material (e.g. dissolved iron) which masks the impact of the original pool of POC_{SSW} on INP concentrations. $\text{INP}_{\text{SSA}, -18^\circ\text{C}}$ are also significantly correlated with $\text{INP}_{\text{SSW}, -16^\circ\text{C}}$ (results not shown), but with a sample size of $n = 4$ this finding requires further validation. Nonetheless, this result could indicate that INP_{SSA} at this tempera-

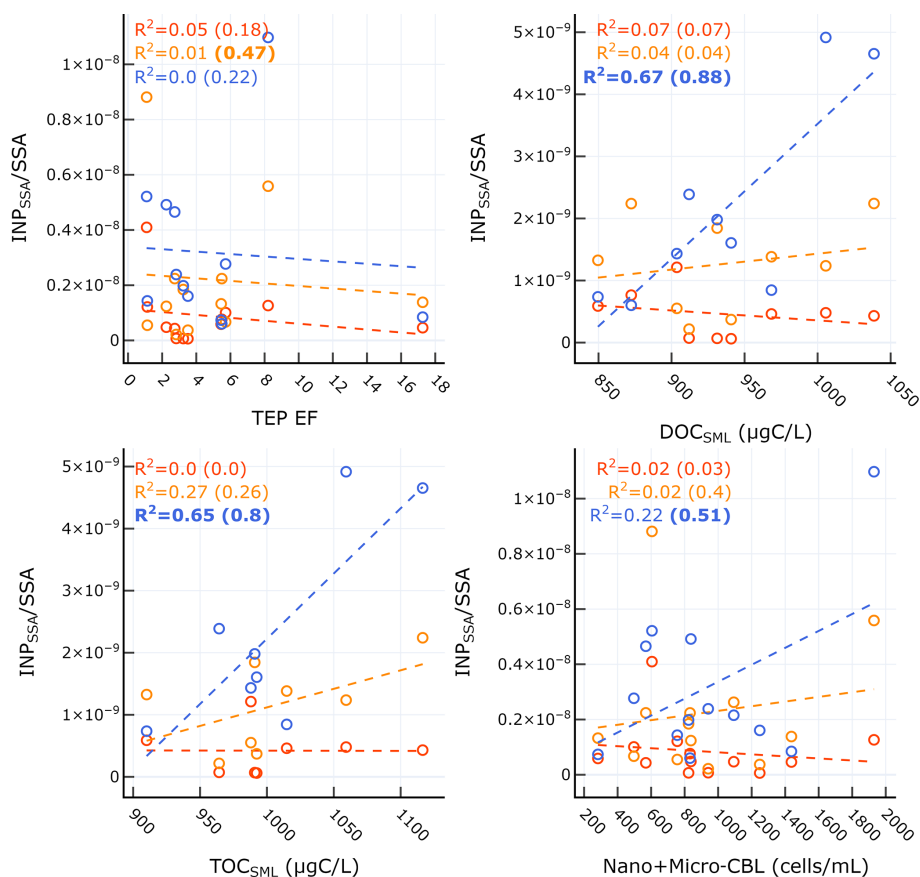


Figure 6. Scatter plots of INP_{SSA} normalized by SSA number concentrations at three temperatures and select conditions in the SML for relationships that were statistically significant. Corresponding correlation parameters are reported Table 2. R^2 values for all days are shown in each plot, with R^2 values for days not including the dust deposition event (i.e. days before 4 June) in parentheses. R^2 for statistically significant relationships are shown in bold.

Table 2. Correlation statistics between INP_{SSA} and properties in the SML, where p is the p -value test for significance and r is the Pearson correlation coefficient. Values in parentheses are calculated for days before the dust deposition event (i.e. days before 4 June). Values that are not statistically significant ($p > 0.05$) are italicized.

Variable	$p_{\text{all days}}$ ($p_{\text{pre-dust}}$)	$r_{\text{all days}}$ ($r_{\text{pre-dust}}$)
–18 °C		
No significant correlations		
–22 °C		
TEP EF	<i>0.80</i> (0.028)	<i>–0.081</i> (0.69)
–25 °C		
DOC _{SML}	0.0071 (0.00055)	0.82 (0.94)
TOC _{SML}	0.016 (0.0066)	0.80 (0.89)
DOC EF	<i>0.45</i> (0.014)	<i>0.29</i> (0.81)
Nano + micro-CBL	<i>0.10</i> (0.021)	<i>0.47</i> (0.71)

ture comes from the bulk water rather than the SML. INP_{SSA} at -22 °C shows a slightly weaker, yet still significant correlation with POC_{SSW} than INP_{SSA} at -18 °C on pre-dust days ($r = 0.54$). Additionally, they have a correlation with *Prochlorococcus*, coccolithophores, and micro-NCBL. This finding is in agreement with a recent study in which particles generated from lysed *Prochlorococcus* cultures exhibited good ice-nucleating capabilities, albeit at much colder temperatures than observed in our study (i.e. $T < -40$ °C; Wolf et al., 2019). INP_{SSA} at -25 °C was correlated with similar variables to INP_{SSA} at -22 °C, with the exception POC_{SSW} . Furthermore, the correlations with the various microbial categories were stronger for INP_{SSA} at -25 °C than at warmer temperatures, indicating these parameters are more associated with cold INPs. Interestingly, INP_{SSA} , -25 °C was not correlated with DOC_{SSW} , yet was correlated with DOC_{SML} (Table 2), potentially indicating an important step in the process of transfer of IN-active DOC material to the atmosphere is its prior enrichment at the SML.

Table 4 and Fig. 8 show the significant correlations between INP_{SSA} and SSA properties. A time series of SSA

Table 3. Correlation statistics between INP_{SSA} and properties in the SSW, where p is the p -value test for significance and r is the Pearson correlation coefficient. Values in parentheses are calculated for days before the dust deposition event (i.e. days before 4 June). Values that are not statistically significant ($p > 0.05$) are italicized.

Variable	$P_{\text{all days}} (P_{\text{pre-dust}})$	$r_{\text{all days}} (r_{\text{pre-dust}})$
–18 °C		
POC_{SSW}	0.95 (0.010)	0.017 (0.64)
DOC_{SSW}	0.16 (0.023)	–0.51 (–0.78)
–22 °C		
Nanoeukaryotes < 10 μm	0.021 (0.050)	–0.51 (–0.48)
<i>Prochlorococcus</i>	0.23 (0.000014)	0.31 (0.90)
POC_{SSW}	0.44 (0.036)	0.20 (0.54)
Coccolithophores	0.67 (0.033)	0.10 (0.52)
Micro-NCBL	0.14 (0.0085)	0.43 (0.77)
–25 °C		
Nanoeukaryotes < 10 μm	0.0065 (0.0042)	–0.59 (–0.65)
<i>Prochlorococcus</i>	0.00033 (0.00014)	0.77 (0.84)
Coccolithophores	0.033 (0.039)	0.48 (0.50)
Cryptophytes	0.034 (0.052)	0.48 (0.48)
Micro-NCBL	0.0013 (0.0053)	0.79 (0.80)
Nano-NCBL	0.049 (0.059)	0.56 (0.61)

chemical properties is shown in Fig. S6 in the Supplement. A positive correlation was observed between $\text{INP}_{\text{SSA},-18\text{C}}$ and SSA OC as well as in the ratio of SSA water-soluble organic carbon to organic carbon (WSOC/OC). The correlation between WSOC/OC and $\text{INP}_{\text{SSA},-18\text{C}}$ makes sense given the finding that $\text{INP}_{\text{SSA},-18\text{C}}$ was correlated with POC_{SSW} . A higher WSOC/OC value would suggest a higher fraction of soluble organics which would be expected to transfer to the atmosphere from the bulk SSW rather than the SML due to their high solubility.

Figure 8 and Table 4 also show that $\text{INP}_{\text{SSA},-25\text{C}}$ had a significant correlation with WIOC and organic mass fraction of sea spray (OMSS) ($r = 0.58$ and $r = 0.65$, respectively). As mentioned above, $\text{INP}_{\text{SSA},-25\text{C}}$ was found to be correlated with various microbes in the SSW, specifically *Prochlorococcus*, coccolithophores, and nano- and micro-NCBL. Phytoplankton are known for their ability to produce extracellular polymeric substances (Thornton, 2014), and a previous mesocosm experiment showed microbially derived long-chain fatty acids were efficiently ejected from the seawater as SSAs, increasing the fraction of highly aliphatic WIOC (Cochran et al., 2017). A separate paper discusses the trend and controls on SSA chemical composition, linking the different classes of organic carbon in submicrometre SSAs to seawater chemical and biological properties (Freny et al., 2020). In this work, OMSS was linked to POC_{SSW} and the coccolithophore cell abundance. In light of this and given the correlation of $\text{INP}_{\text{SSA},-25\text{C}}$ with seawater microbial abundance and with SSA OMSS and WIOC, it seems likely that INP_{SSA} at this temperature is related to the exudates of phy-

Table 4. Correlation statistics between INP_{SSA} and SSA properties, where p is the p -value test for significance and r is the Pearson correlation coefficient. Values in parentheses are calculated for days before the dust deposition event (i.e. days before 4 June). Values that are not statistically significant ($p > 0.05$) are italicized.

Variable	$P_{\text{all days}} (P_{\text{pre-dust}})$	$r_{\text{all days}} (r_{\text{pre-dust}})$
–18 °C		
WSOC/OC	0.0099 (0.014)	0.68 (0.68)
OC	0.018 (0.021)	0.64 (0.65)
WSOC	0.25 (0.0074)	0.29 (0.66)
–22 °C		
WSOC	0.042 (0.0082)	0.48 (0.65)
OC	0.015 (0.0080)	0.66 (0.72)
WIOC	0.061 (0.043)	0.53 (0.59)
OMSS	0.066 (0.028)	0.52 (0.63)
–25 °C		
WIOC	0.037 (0.057)	0.58 (0.56)
OMSS	0.016 (0.025)	0.65 (0.64)

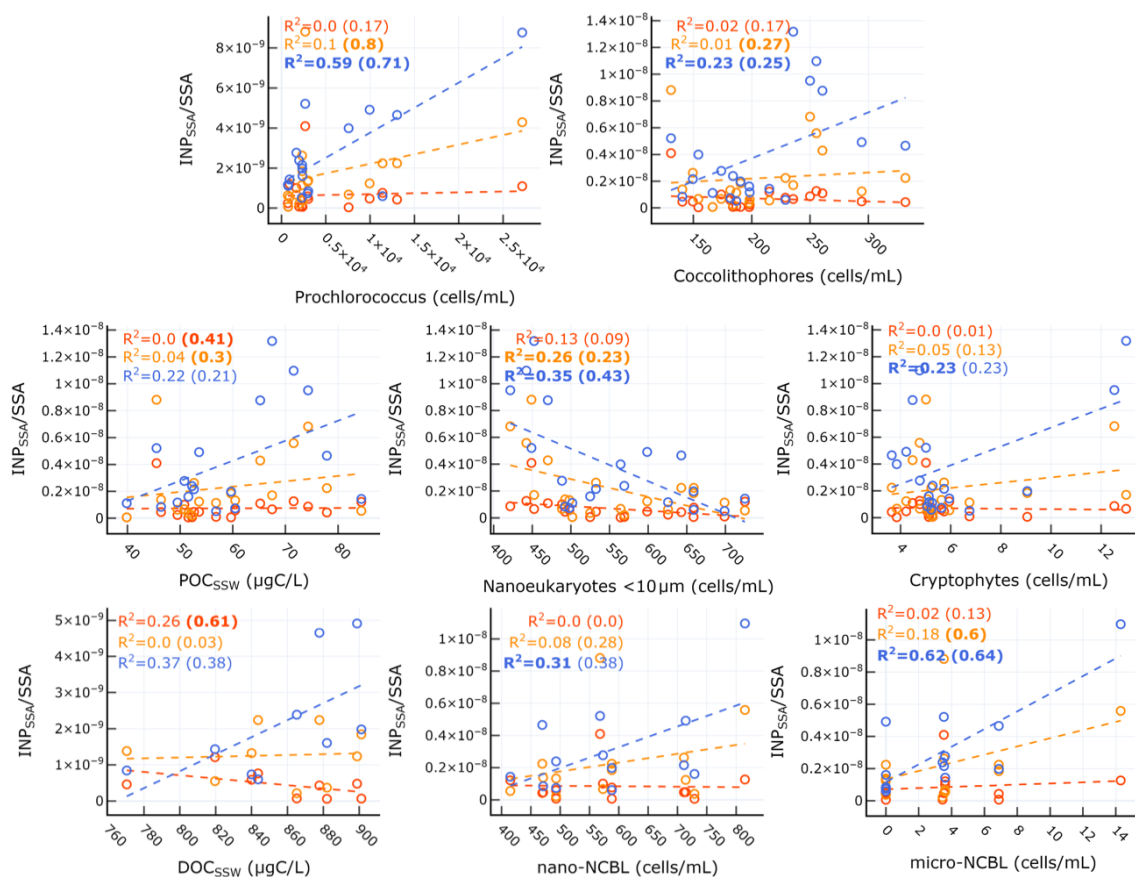


Figure 7. Scatter plots of INP_{SSA} normalized by SSA number concentrations at three temperatures and select conditions in the SSW for relationships that were statistically significant. Corresponding correlation parameters are reported Table 3. R^2 values for all days are shown in each plot, with R^2 values for days not including the dust deposition event (i.e. days before 4 June) in parentheses. R^2 for statistically significant relationships are shown in bold.

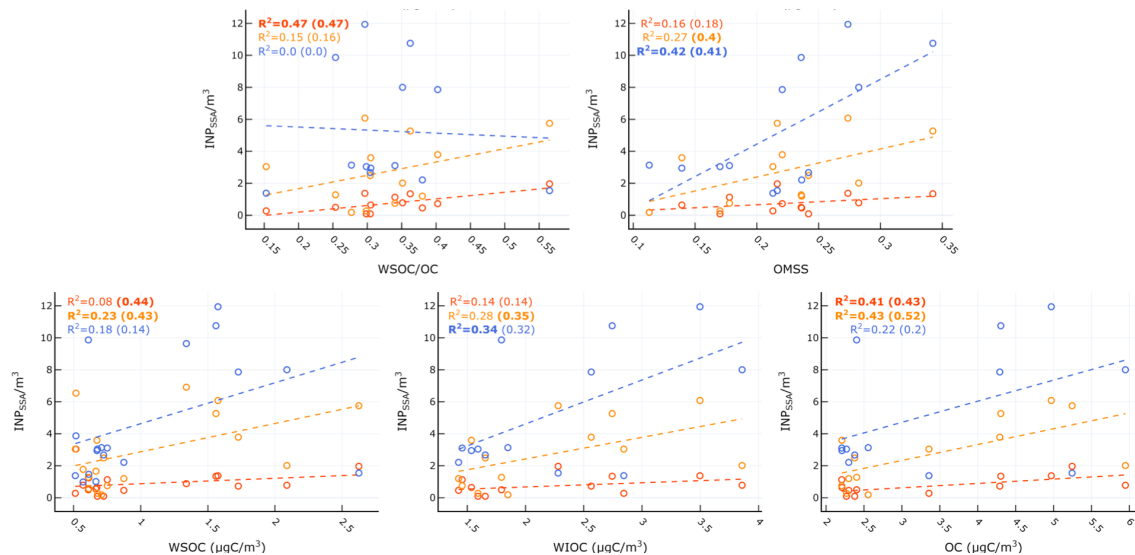


Figure 8. Scatter plots of INP_{SSA} at three temperatures and SSA properties for relationships that were statistically significant. Corresponding correlation statistics s are reported Table 2. R^2 values for all days are shown in each plot, with values calculated before the dust event (i.e. days before 4 June) in parentheses. Statistically significant values are shown in bold.

toplankton which are concentrated at the SML and then emitted into the SSAs as WIOC.

To summarize the results thus far, we have found evidence for the existence of two classes of INPs in SSAs with separate sources: (1) a class of INPs related to POC in the bulk SSW and SSA WIOC and (2) a class of INPs related to microbial abundance and POC in the SSW, DOC in the SML, and WIOC in SSAs. These findings of a two-component marine INP population agree with a recent study which also reported on the existence of dual classes of INPs emitted as SSAs during two mesocosm experiments, described as (1) particulate organic carbon INPs coming from intact cells or IN-active microbe fragments and (2) dissolved organic carbon INPs composed of IN-active molecules enhanced during periods when the SML is enriched with exudates and cellular detritus (McCluskey et al., 2018a). However, in contrast to that study, we report here the existence of separate temperature regimes at which each INP class is active. Here, the first class of INPs consists of INPs that are more active at warmer temperatures ($T = -18\text{ }^{\circ}\text{C}$) while the second class of INPs are active at colder temperatures ($T = -25\text{ }^{\circ}\text{C}$). INPs at $T = -22\text{ }^{\circ}\text{C}$ correlate with items from both warm and cold categories.

4 Proposal of new INP parameterization and comparison with previous models

To date, parameterizations for the estimation of INPs in SSAs have not incorporated the knowledge of a two-component INP population. Rather, they have predicted INPs based on OC or SSA surface area (Wilson et al., 2015, and McCluskey et al., 2018a, respectively). To improve upon existing models, we formulated various parameterizations consisting of different time periods, features, and number of components for temperature ranges. Predictor features were chosen based upon their correlation with INP concentrations as described in the previous section. Single-component parameterizations in which INPs across all three temperatures were linked with the same features were compared with two-component parameterizations in which INPs were split into warm and cold categories, each having their own predictor features. Finally, we developed and compared an altered version of the W15 model to account for the oligotrophic seawater of the Mediterranean Sea, as the existing model was formulated from observations of eutrophic waters. An altered version of the MC18 model for oligotrophy is presented in the Supplement (Fig. S7 in the Supplement), based on calculations of INP concentrations normalized by theoretical total SSA surface area. Each parameterization was recalculated using data across all days of the cruise as well as for only days before the dust deposition event in order to determine the impact of the dust event on the ability to predict INPs. The complete set of parameterizations and their associated fit metrics (R^2 and R^2_{adj}) are given in Table S2 in the Supplement.

Figure 9a shows observed vs. predicted INP_{SSA} for the W15 model. Similar to our results for seawater INPs (Fig. 5), a large overprediction is found relative to our observations when using W15. We also present re-calculated best-fit lines to data using the same features as in W15 (i.e. OC) in order to account for possible changes due to the oligotrophic nature of the Mediterranean Sea. We term this parameterization the altered Wilson fit for oligotrophy, which is given by the following:

$$\frac{\text{INP}}{\text{m}^3} = \exp(-7.332 - (0.2989 \times T) + (0.3792 \times \text{OC}_{\text{SSA}})). \quad (3)$$

The results for this fit are shown in Fig. 9a alongside the results of the original W15 parameterization. The altered model offers an improvement over the original parameterization, with an adjusted R^2 on log-transformed INP abundance of $R^2_{\text{adj}} = 0.59$.

We also tried a range of novel parameterizations based on the observed correlations between INP_{SSA} with seawater and SSA properties. Below we describe two parameterizations which offered good fits to the data. The single-component parameterization assumes the abundance of INPs per SSA particle at each temperature can be predicted from POC_{SSW} concentrations:

$$\frac{\text{INP}}{\text{SSA}} = \exp(-28.6963 - (0.2729 \times T) + (0.0366 \times \text{POC}_{\text{SSW}})). \quad (4)$$

The second parameterization separates INPs into warm and cold classes, where warm INPs ($\geq -22\text{ }^{\circ}\text{C}$) are related to SSA OC and cold INPs ($< -22\text{ }^{\circ}\text{C}$) are related to the concentration of SSA WIOC. This two-component parameterization predicts the concentration of INP m^{-3} through the following equations:

$$\frac{\text{INP}_{T \geq 22\text{ }^{\circ}\text{C}}}{\text{m}^3} = \exp(-7.9857 - (0.3178 \times T) + (0.4643 \times \text{OC}_{\text{SSA}})), \quad (5)$$

$$\frac{\text{INP}_{T < 22\text{ }^{\circ}\text{C}}}{\text{m}^3} = \exp(-6.6606 - (0.2712 \times T) + (0.5755 \times \text{WIOC}_{\text{SSA}})). \quad (6)$$

Figure 9b and c show the results of our single-component model using POC_{SSW} and the two-part model which uses SSA WIOC and OC and considers the separate temperature classes of INPs. The adjusted R^2 for each model on the log-transformed INP abundance were $R^2_{\text{adj}} = 0.402$ for the single-component model using POC_{SSW} and $R^2_{\text{adj}} = 0.60$ for the two-component model using OC and WIOC. This result reveals that the two-component method performs as well as the altered Wilson parameterization. Each parameterization's fit to the data is improved when considering pre-dust

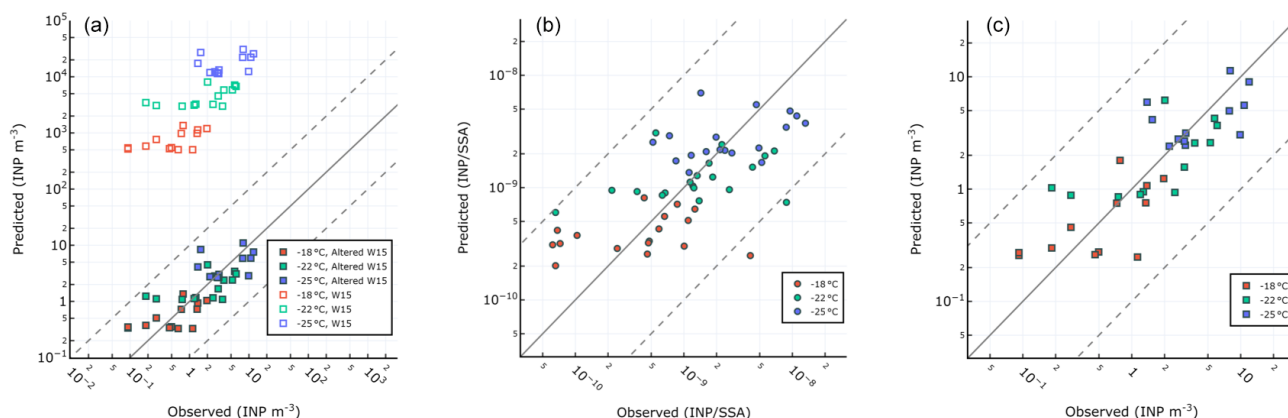


Figure 9. Different parameterizations for prediction of INPs in SSAs. **(a)** W15 and refit of same method using PEACETIME observations. **(b)** Single-component parameterization for INP/SSA where INPs at all temperatures are related to POC_{SSW} . **(c)** Two-component parameterization for INP m^{-3} where $\text{INPs} \geq -22^\circ\text{C}$ are related to OC and $\text{INPs} < -22^\circ\text{C}$ are related to WIOC.

days only ($R_{\text{adj}}^2 = 0.63$ for the two-component parameterization and $R_{\text{adj}}^2 = 0.57$ for the single-component parameterization). The improvement is more pronounced for the single-component parameterization using POC_{SSW} , further pointing to the fact that such dust deposition events can alter the INP properties of surface waters and the subsequent SSAs, either through introduction of terrestrial OC or by triggering changes to the trophic status of the surface waters, resulting in a different class of biologically produced OC. We note that the ratio of $\text{INP}_{\text{SSA}, -18^\circ\text{C}} / \text{OC}_{\text{SSA}}$ is on average $2.08 \times 10^5 \pm 1.4 \times 10^5$ while the ratio of $\text{INP}_{\text{SML}, -15^\circ\text{C}} / \text{TOC}_{\text{SML}}$ as reported in Sect. 3.2.1 is $3.2 \times 10^6 \pm 3.5 \times 10^6 \text{ INP (gC)}^{-1}$. This points to a depletion in the abundance of INP-active material by a factor of 16 as it transfers from the seawater to the SSAs, which is typically assumed to be negligible in modelling studies. However, when available, using a ratio of $\text{INP}_{\text{SSW}} / \text{TOC}_{\text{SSW}}$ to predict sea-spray-originating INPs in the atmosphere seems a better approach than using the ratio $\text{INP}_{\text{SSW}} / \text{NaCl}_{\text{SSW}}$. Finally, we remind the readers that the two-component parameterization uses results of SSA chemistry for submicrometre particles only. As previous studies have shown that the overwhelming majority of SSA OC is found in the submicrometre phase (Gantt and Meskhidze, 2013), we argue that our analysis of WIOC, WSOC, and OC concentrations in submicrometre SSAs is representative of the whole size range of SSAs.

5 Conclusions

In this paper we have presented results from the month-long PEACETIME cruise which took place in the Mediterranean Sea during the spring of 2017, which was characterized with a dust wet deposition event that occurred towards the end of the cruise. We find that the INP concentrations measured in the seawater are in agreement with previous studies on oligotrophic waters (Gong et al., 2020). We next investigated the

relationship between seawater INP concentrations and seawater biogeochemical properties. In the SML, the increase in $\text{INP}_{\text{SML}, -15^\circ\text{C}}$ concentrations during the dust deposition event followed the SML microbial cell counts (e.g. NCBL, CBL, and heterotrophic bacteria), Fe_{SML} , and DOC_{EF} . Excluding this dust event, $\text{INP}_{\text{SML}, -15^\circ\text{C}}$ was still correlated to Fe and bacteria (although not significantly) in the SML. Overall $\text{INP}_{\text{SML}, -15^\circ\text{C}}$ was not correlated with TOC nor DOC in the SML, and compared to previous studies the INP/TOC in the SML observed during the PEACETIME cruise was low. We surmise that this low INP/TOC is a result of TOC from the oligotrophic Mediterranean being less IN active.

The impact of dust deposition on $\text{INP}_{\text{SML}, -15^\circ\text{C}}$ is fairly large, as we observe an increase in $\text{INP}_{\text{SML}, -15^\circ\text{C}}$ by almost an order of magnitude during this event. This impact of dust deposition could have climate implications if $\text{INP}_{\text{SML}, -15^\circ\text{C}}$ were efficiently transferred to the sea spray emitted to the atmosphere. However, we find that INP_{SSA} does not evolve in the same manner as the INP_{SML} does, as an increase in INP_{SSA} is observed with at least a 3-day delay after the dust wet deposition event. This difference could be attributed to the fact that INP_{SSA} measured at -18°C is more influenced by the INP concentration in the bulk surface seawater (as shown by the correlation between $\text{INP}_{\text{SSA}, -18^\circ\text{C}}$ and $\text{INP}_{\text{SSW}, -16^\circ\text{C}}$). It is possible that IN-active species deposited during the rain event, either dust-related or biology-related, take a few days before entering the bulk surface layer.

We also investigated the relationship between INP_{SSA} and various biogeochemical values in the SML, SSW, and SSAs. In general, we observed the existence of two classes of INP_{SSA} , each linked to different classes of organic matter. Our results indicate each class is active at separate temperatures. Warm INPs ($\text{INP}_{\text{SSA}, -18^\circ\text{C}}$) are linked to water-soluble organic matter in the SSAs, but also to SSW parameters (POC_{SSW} $\text{INP}_{\text{SSW}, -16^\circ\text{C}}$). This indicates that INPs at this tem-

perature come from the bulk water rather than the SML. Colder INPs ($\text{INP}_{\text{SSA}, -25\text{C}}$) are rather correlated with SSA water-insoluble organic carbon and SML properties (DOC). As the cold INPs are also correlated to the SSW nano- and micro-NCBL cell abundance as well, we hypothesize that these classes of phytoplankton produce surface-active water-insoluble organic matter that is IN active at these temperatures and is transferred to the atmosphere via the SML. Unfortunately, we do not have measurements of the “colder” temperatures of INPs in the SML to check this hypothesis.

We finally proposed a single-component model linking INP/SSA to POC_{SSW} and a two-component model linking warm INPs to SSA OC and cold INPs to SSA WIOC. Both models utilize features that are readily approximated either from satellite data, biogeochemical models, or from existing parameterizations and observations (Aumont et al., 2015; Rasse et al., 2017; Albert et al., 2010). We then showed these parameterizations fit the data much better than previous single-component model based solely on OC content (W15) developed from studies of more biologically active waters. We also re-calculated parameterizations based on SSA OC content but for the oligotrophic Mediterranean Sea. The parameterization using SSA OC content fits almost as well as the two-component model using SSA OC and WIOC. However, given the results of correlation analysis with SSA properties as well as results from previous studies indicating a dual composition of INPs, we believe the two-component model should help improve attempts to incorporate marine INP emissions into numerical models.

Data availability. Underlying research data are being used by researcher participants of the PEACETIME campaign to prepare other papers, and therefore data are not publicly accessible at the time of publication. The Guieu et al. (2020b) study will be accessible at <https://www.seanoe.org/data/00645/75747/>, once the special issue is completed (all papers should be published by June 2021).

Supplement. The supplement related to this article is available online at: <https://doi.org/10.5194/acp-21-4659-2021-supplement>.

Author contributions. KS designed the emission experiments, and KS and AN performed them. AN performed the seawater, SML, and sea spray aerosol sample INP analysis, with the help of FB and GS. JVT performed the formal INP data analysis and merged data set investigation, with help from KS and EF. BZ and AT-S performed SML sampling and analysed the sample together with ARR. AE, BZ, and ATS contributed to formal analysis of SML data. MR and EF analysed the chemical composition of sea spray aerosol samples. MT, IO, and JD contributed to the analysis of the chemical and biological composition of the SSW. CG contributed to funding acquisition and management of the PEACETIME project. JVT and KS wrote the original draft. All authors contributed to writing and revision of the work.

Competing interests. The authors declare that they have no conflict of interest.

Special issue statement. This article is part of the special issue “Atmospheric deposition in the low-nutrient–low-chlorophyll (LNLC) ocean: effects on marine life today and in the future (ACP/BG inter-journal SI)”. It is not associated with a conference.

Acknowledgements. This study is a contribution to the PEACETIME project (<https://doi.org/10.17600/17000300> and <http://peacetime-project.org>, last access: 19 March 2021), a joint initiative of the MERMEX and ChArMEX projects and to the Sea2Cloud project. The PEACETIME cruise was endorsed as a process study by GEOTRACES and is also a contribution to IMBER and SOLAS. Sea2Cloud is endorsed by SOLAS. We thank the captain and the crew of the R/V *Pourquoi Pas?* for their professionalism and their work at sea. The underway optical instrumentation was provided by Emmanuel Boss’s group.

Financial support. CHARMEX and MERMEX are supported by CNRS-INSU, IFREMER, CEA, and Météo-France as part of the programme MISTRALS coordinated by INSU. The Sea2Cloud project is funded by the European Research Council (ERC) under the European Union’s Horizon 2020 research and innovation program (Sea2Cloud grant agreement no. 771369). Emmanuel Boss’s group is funded by NASA Ocean Biology and Biogeochemistry.

Review statement. This paper was edited by Anne Perring and reviewed by three anonymous referees.

References

- Albert, M. F. M. A., Schaap, M., de Leeuw, G., and Builtjes, P. J. H.: Progress in the determination of the sea spray source function using satellite data, *J. Integr. Environ. Sci.*, 7, 159–166, <https://doi.org/10.1080/19438151003621466>, 2010.
- Aumont, O., Ethé, C., Tagliabue, A., Bopp, L., and Gehlen, M.: PISCES-v2: an ocean biogeochemical model for carbon and ecosystem studies, *Geosci. Model Dev.*, 8, 2465–2513, <https://doi.org/10.5194/gmd-8-2465-2015>, 2015.
- Bigg, E. K.: Ice Nucleus Concentrations in Remote Areas, *J. Atmos. Sci.*, 30, 1153–1157, [https://doi.org/10.1175/1520-0469\(1973\)030%3C1153:INCIRA%3E2.0.CO;2](https://doi.org/10.1175/1520-0469(1973)030%3C1153:INCIRA%3E2.0.CO;2), 1973.
- Burrows, S. M., Hoose, C., Pöschl, U., and Lawrence, M. G.: Ice nuclei in marine air: biogenic particles or dust?, *Atmos. Chem. Phys.*, 13, 245–267, <https://doi.org/10.5194/acp-13-245-2013>, 2013.
- Burrows, S. M., Ogunro, O., Frossard, A. A., Russell, L. M., Rasch, P. J., and Elliott, S. M.: A physically based framework for modeling the organic fractionation of sea spray aerosol from bubble film Langmuir equilibria, *Atmos. Chem. Phys.*, 14, 13601–13629, <https://doi.org/10.5194/acp-14-13601-2014>, 2014.

- Cochran, R. E., Laskina, O., Trueblood, J. V., Estillore, A. D., Morris, H. S., Jayarathne, T., Sultana, C. M., Lee, C., Lin, P., Laskin, J., Laskin, A., Dowling, J. A., Qin, Z., Cappa, C. D., Bertram, T. H., Tivanski, A. V., Stone, E. A., Prather, K. A., and Grassian, V. H.: Molecular Diversity of Sea Spray Aerosol Particles: Impact of Ocean Biology on Particle Composition and Hygroscopicity, *Chem*, 2, 655–667, <https://doi.org/10.1016/j.chempr.2017.03.007>, 2017.
- DeMott, P. J., Hill, T. C. J., McCluskey, C. S., Prather, K. A., Collins, D. B., Sullivan, R. C., Ruppel, M. J., Mason, R. H., Irish, V. E., Lee, T., Hwang, C. Y., Rhee, T. S., Snider, J. R., McMeeking, G. R., Dhaniyala, S., Lewis, E. R., Wentzell, J. J. B., Abbatt, J., Lee, C., Sultana, C. M., Ault, A. P., Axson, J. L., Martinez, M. D., Venero, I., Santos-Figueroa, G., Stokes, D. M., Deane, G. B., Mayol-Bracero, O. L., Grassian, V. H., Bertram, T. H., Bertram, A. K., Moffett, B. F., and Franc, G. D.: Sea Spray Aerosol as a Unique Source of ice Nucleating Particles, *P. Natl. Acad. Sci. USA*, 113, 5797–5803, <https://doi.org/10.1073/pnas.1514034112>, 2016.
- DeMott, P. J., Möhler, O., Cziczko, D. J., Hiranuma, N., Petters, M. D., Petters, S. S., Belosi, F., Bingemer, H. G., Brooks, S. D., Budke, C., Burkert-Kohn, M., Collier, K. N., Danielczok, A., Eppers, O., Felgitsch, L., Garimella, S., Grothe, H., Herenz, P., Hill, T. C. J., Höhler, K., Kanji, Z. A., Kiselev, A., Koop, T., Kristensen, T. B., Krüger, K., Kulkarni, G., Levin, E. J. T., Murray, B. J., Nicosia, A., O'Sullivan, D., Peckhaus, A., Polen, M. J., Price, H. C., Reicher, N., Rothenberg, D. A., Rudich, Y., Santachiara, G., Schiebel, T., Schrod, J., Seifried, T. M., Stratmann, F., Sullivan, R. C., Suski, K. J., Szakáll, M., Taylor, H. P., Ullrich, R., Vergara-Temprado, J., Wagner, R., Whale, T. F., Weber, D., Welti, A., Wilson, T. W., Wolf, M. J., and Zenker, J.: The Fifth International Workshop on Ice Nucleation phase 2 (FIN-02): laboratory intercomparison of ice nucleation measurements, *Atmos. Meas. Tech.*, 11, 6231–6257, <https://doi.org/10.5194/amt-11-6231-2018>, 2018.
- Engel, A.: Determination of Marine Gel Particles, in: *Practical Guidelines for the Analysis of Seawater*, edited by: Wurl, O., CRC Press Taylor & Francis Group, Boca Raton, FL, 125–142, 2009.
- Franklin, C. N., Z. Sun, D. B., Yan, M. D. H., and Bodas-Salcedo, A.: Evaluation of Clouds in ACCESS Using the Satellite Simulator Package COSP: Global, Seasonal, and Regional Cloud Properties, *J. Geophys. Res.-Atmos.*, 118, 732–748, <https://doi.org/10.1029/2012JD018469>, 2013.
- Frenay, E., Sellegri, K., Nicosia, A., Trueblood, J. T., Rinaldi, M., Williams, L. R., Prévôt, A. S. H., Thyssen, M., Grégori, G., Haëntjens, N., Dinasquet, J., Obernosterer, I., Van-Wambeke, F., Engel, A., Zäncker, B., Desboeufs, K., Asmi, E., Timmonen, H., and Guieu, C.: Mediterranean nascent sea spray organic aerosol and relationships with seawater biogeochemistry, *Atmos. Chem. Phys. Discuss.* [preprint], <https://doi.org/10.5194/acp-2020-406>, in review, 2020.
- Fuentes, E., Coe, H., Green, D., de Leeuw, G., and McFiggans, G.: Laboratory-generated primary marine aerosol via bubble-bursting and atomization, *Atmos. Meas. Tech.*, 3, 141–162, <https://doi.org/10.5194/amt-3-141-2010>, 2010.
- Gantt, B. and Meskhidze, N.: The physical and chemical characteristics of marine primary organic aerosol: a review, *Atmos. Chem. Phys.*, 13, 3979–3996, <https://doi.org/10.5194/acp-13-3979-2013>, 2013.
- Gong, X., Wex, H., van Pinxteren, M., Triesch, N., Fomba, K. W., Lubitz, J., Stolle, C., Robinson, T.-B., Müller, T., Herrmann, H., and Stratmann, F.: Characterization of aerosol particles at Cabo Verde close to sea level and at the cloud level – Part 2: Ice-nucleating particles in air, cloud and seawater, *Atmos. Chem. Phys.*, 20, 1451–1468, <https://doi.org/10.5194/acp-20-1451-2020>, 2020.
- Guieu, C., D'Ortenzio, F., Dulac, F., Taillandier, V., Doglioli, A., Petrenko, A., Barrillon, S., Mallet, M., Nabat, P., and Desboeufs, K.: Introduction: Process studies at the air–sea interface after atmospheric deposition in the Mediterranean Sea – objectives and strategy of the PEACETIME oceanographic campaign (May–June 2017), *Biogeosciences*, 17, 5563–5585, <https://doi.org/10.5194/bg-17-5563-2020>, 2020a.
- Guieu, C., Desboeufs, K., Albani, S., et al.: Biogeochemical dataset collected during the PEACETIME cruise, available at: <https://www.seanoe.org/data/00645/75747/>, 2020b.
- Hiranuma, N., Adachi, K., Bell, D. M., Belosi, F., Beydoun, H., Bhaduri, B., Bingemer, H., Budke, C., Clemen, H.-C., Conen, F., Cory, K. M., Curtius, J., DeMott, P. J., Eppers, O., Grawe, S., Hartmann, S., Hoffmann, N., Höhler, K., Jantsch, E., Kiselev, A., Koop, T., Kulkarni, G., Mayer, A., Murakami, M., Murray, B. J., Nicosia, A., Petters, M. D., Piazza, M., Polen, M., Reicher, N., Rudich, Y., Saito, A., Santachiara, G., Schiebel, T., Schill, G. P., Schneider, J., Segev, L., Stopelli, E., Sullivan, R. C., Suski, K., Szakáll, M., Tajiri, T., Taylor, H., Tobo, Y., Ullrich, R., Weber, D., Wex, H., Whale, T. F., Whiteside, C. L., Yamashita, K., Zelenyuk, A., and Möhler, O.: A comprehensive characterization of ice nucleation by three different types of cellulose particles immersed in water, *Atmos. Chem. Phys.*, 19, 4823–4849, <https://doi.org/10.5194/acp-19-4823-2019>, 2019.
- Irish, V. E., Elizondo, P., Chen, J., Chou, C., Charette, J., Lizotte, M., Ladino, L. A., Wilson, T. W., Gosselin, M., Murray, B. J., Polishchuk, E., Abbatt, J. P. D., Miller, L. A., and Bertram, A. K.: Ice-nucleating particles in Canadian Arctic sea-surface microlayer and bulk seawater, *Atmos. Chem. Phys.*, 17, 10583–10595, <https://doi.org/10.5194/acp-17-10583-2017>, 2017.
- Irish, V. E., Hanna, S. J., Xi, Y., Boyer, M., Polishchuk, E., Ahmed, M., Chen, J., Abbatt, J. P. D., Gosselin, M., Chang, R., Miller, L. A., and Bertram, A. K.: Revisiting properties and concentrations of ice-nucleating particles in the sea surface microlayer and bulk seawater in the Canadian Arctic during summer, *Atmos. Chem. Phys.*, 19, 7775–7787, <https://doi.org/10.5194/acp-19-7775-2019>, 2019.
- Knopf, D. A., Alpert, P. A., Wang, B., and Aller, J. Y.: Stimulation of Ice Nucleation by Marine Diatoms, *Nat. Geosci.*, 4, 88–90, <https://doi.org/10.1038/ngeo1037>, 2011.
- McCluskey, C. S., Hill, T. C. J., Malfatti, F., Sultana, C. M., Lee, C., Santander, M. V., Beall, C. M., Moore, K. A., Cornwall, G. C., Collins, D. B., Prather, K. A., Jayarathne, T., Stone, E. A., Azam, F., Kreidenweis, S. M., and DeMott, P. J.: A Dynamic Link between Ice Nucleating Particles Released in Nascent Sea Spray Aerosol and Oceanic Biological Activity during Two Mesocosm Experiments, *J. Atmos. Sci.*, 74, 151–166, <https://doi.org/10.1175/JAS-D-16-0087.1>, 2017.
- McCluskey, C. S., Hill, T. C. J., Sultana, C. M., Laskina, O., Trueblood, J. V., Santander, M. V., Beall, C. M., Michaud, J. M.,

- Kreidenweis, S. M., Prather, K. A., Grassian, V. H., and DeMott, P. J.: A Mesocosm Double Feature: Insights into the Chemical Makeup of Marine Ice Nucleating Particles, *J. Atmos. Sci.*, 75, 2405–2423, <https://doi.org/10.1175/JAS-D-17-0155.1>, 2018a.
- McCluskey, C. S., Ovadnevaite, J., Rinaldi, M., Atkinson, J., Berosi, F., Ceburnis, D., Marullo, S., Hill, T. C. J., Lohmann, U., Kanji, Z. A., O’Dowd, C., Kreidenweis, S. M., and DeMott, P. J.: Marine and Terrestrial Organic Ice-Nucleating Particles in Pristine Marine to Continentally Influenced Northeast Atlantic Air Masses, *J. Geophys. Res.-Atmos.*, 123, 6196–6212, <https://doi.org/10.1029/2017JD028033>, 2018b.
- McCluskey, C. S., DeMott, P. J., Ma, P. L., and Burrows, S. M.: Numerical Representations of Marine Ice-Nucleating Particles in Remote Marine Environments Evaluated Against Observations, *Geophys. Res. Lett.*, 46, 7838–7847, <https://doi.org/10.1029/2018GL081861>, 2019.
- McCoy, D. T., Hartmann, D. L., Zelinka, M. D., Ceppi, P., and Grosvenor, D. P.: Mixed-phase Cloud Physics and Southern Ocean Cloud Feedback in Climate Models, *J. Geophys. Res.-Atmos.*, 120, 9539–9554, <https://doi.org/10.1175/JAS-D-17-0155.1>, 2015.
- McCoy, D. T., Tan, I., Hartmann, D. L., Zelinka, M. D., and Storelvmo, T.: On the Relationship Among Cloud Cover, Mixed-phase Partitioning and Planetary Albedo in GCMs, *J. Adv. Model. Earth Syst.*, 8, 650–668, <https://doi.org/10.1002/2015MS000589>, 2016.
- Ovadnevaite, J., Manders, A., de Leeuw, G., Ceburnis, D., Monahan, C., Partanen, A.-I., Korhonen, H., and O’Dowd, C. D.: A sea spray aerosol flux parameterization encapsulating wave state, *Atmos. Chem. Phys.*, 14, 1837–1852, <https://doi.org/10.5194/acp-14-1837-2014>, 2014.
- Pujo-Pay, M., Conan, P., Oriol, L., Cornet-Barthaux, V., Falco, C., Ghiglione, J.-F., Goyet, C., Moutin, T., and Prieur, L.: Integrated survey of elemental stoichiometry (C, N, P) from the western to eastern Mediterranean Sea, *Biogeosciences*, 8, 883–899, <https://doi.org/10.5194/bg-8-883-2011>, 2011.
- Rasse, R., Dall’Olmo, G., Graff, J., Westberry, T. K., van Dongen-Vogels, V., and Behrenfeld, M. J.: Evaluating Optical Proxies of Particulate Organic Carbon across the Surface Atlantic Ocean, *Front. Mar. Sci.*, 4, 367, 2017.
- Rogers, D. C., DeMott, P. J., Kreidenweis, S. M., and Chen, Y.: Measurements of Ice Nucleating Aerosols During SUCCESS, *Geophys. Res. Lett.*, 25, 1383–1386, <https://doi.org/10.1029/97GL03478>, 1998.
- Schnell, R. C. and Vali, G.: Biogenic ice Nuclei: Part I. Terrestrial and Marine Sources, *J. Atmos. Sci.*, 33, 1554–1564, [https://doi.org/10.1175/1520-0469\(1976\)033<1554:BINPIT>2.0.CO;2](https://doi.org/10.1175/1520-0469(1976)033<1554:BINPIT>2.0.CO;2), 1976.
- Schwier, A. N., Rose, C., Asmi, E., Ebling, A. M., Landing, W. M., Marro, S., Pedrotti, M.-L., Sallon, A., Iuculano, F., Agusti, S., Tsiola, A., Pitta, P., Louis, J., Guieu, C., Gazeau, F., and Sellegri, K.: Primary marine aerosol emissions from the Mediterranean Sea during pre-bloom and oligotrophic conditions: correlations to seawater chlorophyll *a* from a mesocosm study, *Atmos. Chem. Phys.*, 15, 7961–7976, <https://doi.org/10.5194/acp-15-7961-2015>, 2015.
- Schwier, A. N., Sellegri, K., Mas, S., Charrière, B., Pey, J., Rose, C., Temime-Roussel, B., Jaffrezo, J.-L., Parin, D., Picard, D., Ribeiro, M., Roberts, G., Sempéré, R., Marchand, N., and D’Anna, B.: Primary marine aerosol physical flux and chemical composition during a nutrient enrichment experiment in mesocosms in the Mediterranean Sea, *Atmos. Chem. Phys.*, 17, 14645–14660, <https://doi.org/10.5194/acp-17-14645-2017>, 2017.
- Stopelli, E., Conen, F., Zimmermann, L., Alewell, C., and Morris, C. E.: Freezing nucleation apparatus puts new slant on study of biological ice nucleators in precipitation, *Atmos. Meas. Tech.*, 7, 129–134, <https://doi.org/10.5194/amt-7-129-2014>, 2014.
- Thornton, D. C. O.: Dissolved organic matter (DOM) release by phytoplankton in the contemporary and future ocean, *Eur. J. Phycol.*, 49, 20–46, <https://doi.org/10.1080/09670262.2013.875596>, 2014.
- Tovar-Sanchez, A., Arrieta, J. M., Duarte, C. M., and Sanudo-Wilhelmy, S. A.: Spatial Gradients in Trace Metal Concentrations in the Surface Microlayer of the Mediterranean Sea, *Front. Mar. Sci.*, 1, 1–8, <https://doi.org/10.3389/fmars.2014.00079>, 2019.
- Vali, G.: Quantitative Evaluation of Experimental Results on the Heterogeneous Freezing Nucleation of Supercooled Liquids, *J. Atmos. Sci.*, 28, 402–409, 1971.
- Vali, G., DeMott, P. J., Möhler, O., and Whale, T. F.: Technical Note: A proposal for ice nucleation terminology, *Atmos. Chem. Phys.*, 15, 10263–10270, <https://doi.org/10.5194/acp-15-10263-2015>, 2015.
- Vergara-Temprado, J., Murray, B. J., Wilson, T. W., O’Sullivan, D., Browse, J., Pringle, K. J., Ardon-Dryer, K., Bertram, A. K., Burrows, S. M., Ceburnis, D., DeMott, P. J., Mason, R. H., O’Dowd, C. D., Rinaldi, M., and Carslaw, K. S.: Contribution of feldspar and marine organic aerosols to global ice nucleating particle concentrations, *Atmos. Chem. Phys.*, 17, 3637–3658, <https://doi.org/10.5194/acp-17-3637-2017>, 2017.
- Verheggen, B., Cozic, J., Weingartner, E., Bower, K., Mertes, S., Connolly, P., Gallagher, M., Flynn, M., Choulaton, T., and Baltensperger, U.: Aerosol Partitioning Between the Interstitial and the Condensed Phase in Mixed-phase Clouds, *J. Geophys. Res.*, 112, 2156–2202, <https://doi.org/10.1029/2007JD008714>, 2007.
- Wilson, T. W., Ladino, L. A., Alpert, P. A., Breckels, M. N., Brooks, I. M., Browse, J., Burrows, S. M., Carslaw, K. S., Huffman, J. A., Judd, C., Kilhau, W. P., Mason, R. H., McFiggans, G., Miller, L. A., Nájera, J. J., Polishchuk, E., Rae, S., Schiller, C. L., Si, M., Vergara Temprado, J., Whale, T. F., Wong, J. P. S., Wurl, O., Yakobi-Hancock, J. D., Abbatt, J. P. D., Aller, J. Y., Bertram, A. K., Knopf, D. A., and Murray, D. J.: A Marine Biogenic Source of Atmospheric Ice-Nucleating Particles, *Nature*, 525, 234–238, <https://doi.org/10.1038/nature14986>, 2015.
- Wolf, M. J., Coe, A., Dove, L. A., Zawadowicz, M. A., Doolley, K., Biller, S. J., Zhang, Y., Chisholm, S. W., and Cziczo, D. J.: Investigating the Heterogeneous Ice Nucleation of Sea Spray Aerosols Using *Prochlorococcus* as a Model Source of Marine Organic Matter, *Environ. Sci. Technol.*, 53, 1139–1149, <https://doi.org/10.1021/acs.est.8b05150>, 2019.